Hindawi
International Journal of Corrosion
Volume 2018, Article ID 9471694, 10 pages
https://doi.org/10.1155/2018/9471694

*Research Article*

# Prevention of Reinforcement Corrosion in Concrete by Sodium Lauryl Sulphate: Electrochemical and Gravimetric Investigations

**Binsi M. Paulson,[1] Thomas K. Joby,[1] Vinod P. Raphael,[2] and K. S. Shaju[2]**

[1]*Research Division, Dept. of Chemistry, St. Thomas' College (Autonomous), Thrissur, Kerala 680001, India*
[2]*Dept. of Chemistry, Government Engineering College, Thrissur, Kerala 680009, India*

Correspondence should be addressed to Thomas K. Joby; drjobythomask@gmail.com

Received 24 August 2018; Revised 27 October 2018; Accepted 13 November 2018; Published 2 December 2018

Academic Editor: Ramazan Solmaz



Prolonged corrosion inhibition response of sodium lauryl sulphate (SLS) on steel reinforcement in contaminated concrete was investigated by gravimetric method and electrochemical techniques such as potentiodynamic polarization and electrochemical impedance spectroscopy. Using half cell potential measurements probability of steel reinforcement corrosion was monitored for a period of 480 days. FT-IR spectroscopic analysis of the corroded products deposited on the steel reinforcement revealed the mechanism of corrosion inhibition. Modification in the surface morphology of steel specimens in the concrete was examined by optical microscopy. During the period of investigation (480 days), SLS showed appreciable corrosion inhibition efficiency on the steel reinforcement in concrete.

## 1. Introduction

Reinforced concrete structures are developed to ensure the strength and existence throughout their lifetime. But the deterioration and collapse of reinforced concrete structure are a major issue in construction field [1–3]. $CO_2$ from the air and chloride ions from the sea atmosphere enter into the concrete and make the concrete interstitial solution more aggressive than before [4–8]. Depassivation of the steel reinforcement occurs locally in the presence of chloride ions leading to pitting corrosion [9–12]. Passivation of steel reinforcement takes place due to the alkaline compounds present in the concrete. The cost of replacing deteriorated concrete structures may affect the GDP (Gross Domestic Product) of a country. To find out an effective and economic method to combat the steel reinforcement corrosion in concrete has been attracted by the researchers and engineers for the last two decades.

Addition of the corrosion inhibitors to the concrete mixture is the most practical way to minimize steel reinforcement corrosion in contaminated concrete [13–16]. In ideal situations, corrosion inhibitors will not affect the properties of the concrete. Some of the previous researchers have been established that inhibitor molecules generally affect the kinetics of electrochemical process of corrosion of steel [17–19]. The mechanism of corrosion inhibition by the added compounds may include lowering of the rate of diffusion of chloride ion, enhancing the threshold value of chloride ion, and lowering the rate of anodic and cathodic process of corrosion [20–22]. Corrosion inhibitors can be added to the fresh concrete as an admixture during concrete casting step or can be applied on the concrete surface.

Commercially available corrosion inhibitors may contain either organic or inorganic compounds like sodium nitrite, sodium monofluorophosphate, aminoethanols, and so forth [23–27]. Nowadays, use of nitrites is not recommended due to its toxicity. The efficacies of organic inhibitors are sometimes questionable at elevated chloride concentrations. Researchers, scientists, and engineers are always in search of potent, economic, and environmental-friendly admixtures to combat steel reinforcement corrosion in concrete. Some recently invented green inhibitors like silver nanoparticle doped palm oil leaf extracts [28] and naturally obtained Welan gum and Neem gum [29] have predominant concrete corrosion inhibition efficiency.

Present investigation was conducted to check the corrosion preventing capacity of SLS on steel reinforcement

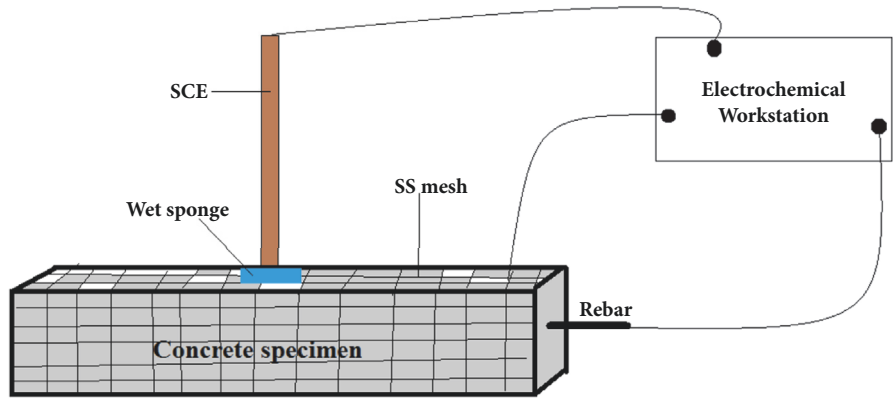


Figure 1: Three-electrode circuitry for electrochemical studies.

in contaminated concrete [30, 31]. Preliminary examinations were done by measuring the electrode potentials of steel reinforcements (against SCE) dipped in concrete pore solution contaminated with 3.5% NaCl containing various concentrations of SLS. After this examination, we decided to investigate the corrosion response of steel reinforcement in concrete specimen containing 2.5% of SLS by weight of cement.

## 2. Experimental

*2.1. Materials.* Sodium lauryl sulphate and sodium chloride (>99.9 %) were procured from Merck Millipore. Portland cement (Indiana Cements, Grade 53) used for making concrete specimens was purchased from the market.

*2.2. Preparation of Concrete Test Specimens.* Concrete blocks containing steel reinforcement used for the experiment were made of Portland cement, coarse aggregate, fine aggregate (sand), and water. Each rectangular block having dimension of 200x80x80mm was prepared by mixing water and cement in the ratio 0.5. The ratio between cement, fine aggregate, and coarse aggregate was 1:1.5:3, which will exactly mimic M-20 grade concrete. SLS was added to the concrete mixture by 2.5 wt% of cement and two test specimens were casted. In this work, we designate the concrete specimen without SLS as SAMPLE 1 and with SLS as SAMPLE 2. The approximate composition of steel rod was estimated by EDAX method: 0.1 % P, 0.62 % Mn, 0.021 % Si, 0.04 % S, and rest Fe. Steel rebars were cut (22 cm) and immersed in 2M HCl for 10 minutes for removing the rust, washed with distilled water, degreased with acetone, dried, weighed, and used as the reinforcement in concrete. After a period of 24 h, the test specimens were removed from the mould and cured for 30 days for the proper hydration and setting of the cement.

*2.3. Treatment of Test Specimens.* After the curing period, five sides of the test specimens were coated with epoxy resin and one open reservoir (100x40x20mm) was built on the remaining side with polypropylene and silicon adhesive. 25mL 3.5% NaCl was added to the reservoir of the specimens and kept for 2 days. This will ensure the complete diffusion of NaCl throughout the specimen. This process was repeated three times during 30-60 days.

*2.4. Electrochemical Investigations*

*(i) Potentiodynamic Polarization Studies.* Figure 1 shows the schematic diagram of the test specimen and the experimental setup for electrochemical studies. Three-electrode cell assembly consisting of steel reinforcement present in concrete as working electrode, concrete specimen covered with a stainless steel mesh as counter electrode, and saturated calomel electrode (SCE) as reference electrode were used for the electrochemical studies [32]. For good electrical contact, a wet sponge was used on the concrete surface between SCE and concrete surface.

After curing and treatment of test specimens with NaCl, polarization studies were performed three times during a period of 480 days in 160 days' interval. Steel reinforcement in the concrete was scanned for a potential range of +250 to -250 mV having a scan rate of 1mV/s. Tafel curves were analyzed to get the slopes, which are extrapolated to get the corrosion current densities. The corrosion inhibition efficiency of SLS was determined using the following equation:

$$\eta_{\text{pol}}\% = \frac{I_{\text{corr}} - I'_{\text{corr}}}{I_{\text{corr}}} \text{X100} \quad (1)$$

where $I_{\text{corr}}$ and $I'_{\text{corr}}$ are corrosion current densities of steel reinforcement in test specimens in the absence and presence of SLS, respectively. Experiments were repeated with the duplicate concrete block and the average values were taken.

*(ii) Electrochemical Impedance Spectroscopic (EIS) Studies.* EIS experiments were carried out at constant potential in the frequency range of 1 KHz to 100 mHz with excitation signal of 10mV amplitude. Analysis of the Nyquist curves using the equivalent circuit gave the charge transfer resistance ($R_{ct}$).

Table 1: Tafel data of steel reinforcement in concrete in the presence and absence of SLS for different periods.

| Time (day) | System | $I_{corr}$ ($\mu A/cm^2$) | $b_a$ (mV/dec) | $-b_c$ (mV/dec) | $-E_{corr}$ (mV) | $\eta_{pol}$ % |
|---|---|---|---|---|---|---|
| 160 | SAMPLE 1 | 161 | 496 | 159 | 651 | |
| | SAMPLE 2 | 18 | 430 | 232 | 573 | 89 |
| 320 | SAMPLE 1 | 139 | 489 | 156 | 662 | |
| | SAMPLE 2 | 41 | 469 | 229 | 520 | 71 |
| 480 | SAMPLE 1 | 107 | 373 | 215 | 551 | |
| | SAMPLE 2 | 21 | 341 | 230 | 561 | 80 |

Using $R_{ct}$ values corrosion inhibition efficacy of SLS was determined using the following equation:

$$\eta_{EIS}\% = \frac{R'_{ct} - R_{ct}}{R_{ct}} X100 \quad (2)$$

where $R'_{ct}$ and $R_{ct}$ are the charge transfer resistance of working electrode with and without SLS, respectively. Polarization and EIS analyses were done using Ivium CompactStat electrochemical work station (IviumSoft).

*(iii) Half Cell Potential Measurements*. For understanding the corrosion response of steel reinforcement in concrete, half cell potential measurements were carried out using saturated calomel electrode (SCE) and high impedance voltmeter (HP E2378A). In this electrochemical cell, steel reinforcement and SCE were acted as anode and cathode, respectively. The potential of the steel rebar was obtained by deducting the cell potential from the standard electrode potential of saturated calomel electrode. Sixteen readings were taken with a regular interval of 1 reading per month during 480 days.

*2.5. Gravimetric Method.* Before casting the concrete blocks, each steel rebar was pickled with 2M HCl for 10 minutes, washed with water, degreased with acetone, dried, and weighed. The surface areas of all reinforcements were the same (10.5$cm^2$). After 480 days, concrete blocks were broken and the steel reinforcements were taken outside, pickled using 2M HCl for 15 minutes to remove the adhered rust, washed with water, dried, and weighed. From the weight loss of the steel specimens, approximate corrosion inhibition efficiency of SLS was calculated by the following equation:

$$\eta\% = \frac{w_0 - w}{w_0} \times 100 \quad (3)$$

where $w_0$ and w are the weight loss of steel rebars of SAMPLE 1 and SAMPLE 2.

*2.6. Spectroscopic Studies.* Fourier Transform Infrared (FT-IR) spectroscopic study of corroded product on the steel reinforcement was conducted using KBr pellet method. The spectrum was recorded in the range of 400-4000$cm^{-1}$ using Shimadzu IR Affinity-1 model FT-IR spectrophotometer.

*2.7. Microscopic Surface Analysis.* After 480 days of electrochemical investigation, the steel specimens were taken outside from the concrete and analyzed using a high-resolution optical microscope (Leica Stereo Microscope, No. S8ACO). This study mainly aims to understand the surface modifications that occurred for steel specimen during the period of investigation.

## 3. Results and Discussions

*3.1. Potentiodynamic Polarization Studies.* The inhibition efficacy of SLS and site of corrosion inhibition on steel reinforcement in the contaminated concrete was monitored using potentiodynamic polarization studies. Analysis of polarization curve gave Tafel slopes, current densities, and percentage of inhibition efficiency which are given in Table 1. From the data, it is understandable that the steel reinforcement in the concrete containing SLS was less corroded than reinforcement in the SAMPLE 1. During 480 days, three sets of measurements were taken in 160 days' interval. It was noticed that SLS exhibited 89% corrosion inhibition efficiency on $160^{th}$ day of study. On $320^{th}$ and $480^{th}$ days of investigation, inhibition efficiency changed to 71% and 80%, respectively. From these results, it can be assured that SLS can act as an efficient admixture, which resists the steel reinforcement corrosion in the contaminated concrete structures for a long time. SLS mainly acted on cathodic sites of corrosion up to 2/3 rd period of investigation, since the cathodic slopes of the Tafel lines altered appreciably (Figure 2). But the corrosion inhibition response of SLS was changed into mixed type (affecting both anodic and cathodic sites) towards the end of study.

The gradation in the inhibition efficiency of SLS can be explained with the help of following hypothesis. The entire period of investigation can be divided into three stages: first stage (0-160 days), second stage (161-320 days), and third stage (321-480 days). In the first stage, SLS molecules adjacent to the steel rebar make coordinate bonds with ferrous ions and prevent chloride ions and water molecules diffusing towards the steel surface considerably. Thus, during this period, SLS protects well the corrosion of reinforcement. Towards the end of second stage (320 days), it was observed that the rate of corrosion slightly increased. Since the rate of diffusion of chloride ion is greater than that of SLS, higher percentage of chloride ions can be expected near the steel surface than that of first stage. The porous nature of the hydrated ferric oxide helps to enter water molecules, chloride, and oxygen more towards the steel surface. Thus SLS showed less corrosion

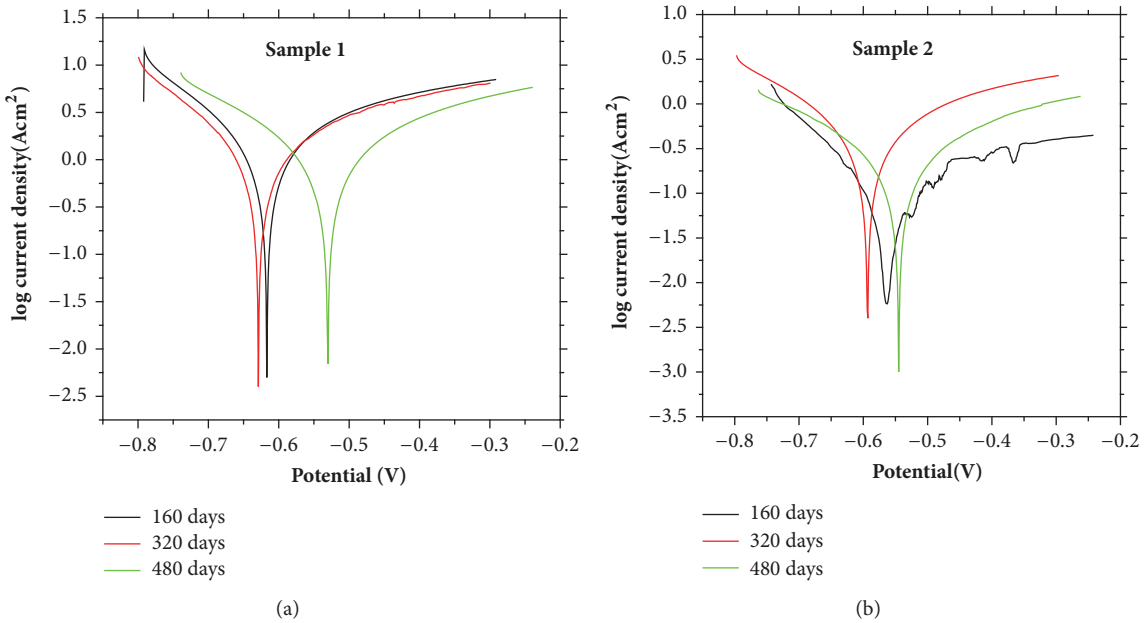


Figure 2: Tafel curves of steel reinforcement in concrete (a) in the absence and (b) presence of SLS for 160, 320, and 480 days.

Table 2: EIS parameters of steel reinforcement in concrete in the presence and absence of inhibitor for different periods.

| Time (day) | Sample | W (Ohmsqrt(Hz) | $R_s$ ($\Omega cm^2$) | $C_{dl}$ ($\mu Fcm^{-2}$) | $R_{ct}$ ($\Omega cm^2$) | $\eta$% |
|---|---|---|---|---|---|---|
| 160 | SAMPLE 1 | 2.74 | 78.5 | 110 | 11.9 | |
| | SAMPLE 2 | 50.2 | 97.5 | 109 | 93.1 | 87.2 |
| 320 | SAMPLE 1 | 3.52 | 157 | 88.5 | 14.7 | |
| | SAMPLE 2 | 9.27 | 459 | 4.2 | 66.5 | 78 |
| 480 | SAMPLE 1 | 3.23 | 223 | 27.3 | 24.3 | |
| | SAMPLE 2 | 15.8 | 574 | 0.96 | 173 | 86 |

protection efficacy at this stage. In the third stage (480 days), the rate of corrosion was seemed to decrease again (but not as that much of first stage). During the end of this stage, it can be believed that more and more SLS molecules migrated towards the steel surface from the bulk and make more coordinate bonds with ferrous ions and protect steel surface. This led to higher corrosion protection efficiency of SLS than in second stage.

*3.2. EIS Measurements.* The corrosion response of steel reinforcement in concrete in the presence and absence of SLS was monitored using electrochemical impedance spectroscopy and the corresponding Nyquist plots are represented in Figure 3. The corrosion behaviour of steel reinforcement was significantly differed in the presence and absence of inhibitor. The equivalent circuit fitted for EIS measurements (Figure 4) consists of solution resistance ($R_s$) which is connected in series to double layer capacitance ($C_1$) and this combination is connected in parallel to a series combination of Warburg resistance (W) and charge transfer resistance ($R_{ct}$) [33, 34]. The EIS parameters of the test specimens are given in Table 2. Impedance data show that addition of SLS leads to the decrease in double-layer capacitance and increase of charge transfer resistance. This is due to the adsorption of SLS molecules on the steel rebar. SLS exhibited 87.2% corrosion inhibition efficiency on 160$^{th}$ day of investigation. Inhibition efficiencies changed to 78 and 86%, respectively, on the 320$^{th}$ and 480$^{th}$ days of study.

*3.3. Half Cell Potential Measurements.* The probability of corrosion of steel reinforcement in concrete was visualized with the help of half cell potential measurements. It was established by the previous researchers that tendency of corrosion increases as the potential of the steel reinforcement changes to more anodic side. Half cell potentials (Vs SCE) of steel reinforcements in concrete blocks during 480 days were measured at a time interval of 30 days and are given in Table 3. The half cell potential values are compared with the help of a line graph and are represented in Figure 5. Data show that the steel reinforcement in concrete block (SAMPLE 1) exhibited high anodic potential values, which is a clear reflection of high corrosion rate in the contaminated concrete. Half cell potentials of steel specimen in SAMPLE 2 were less negative (more cathodic) than SAMPLE 1 during the

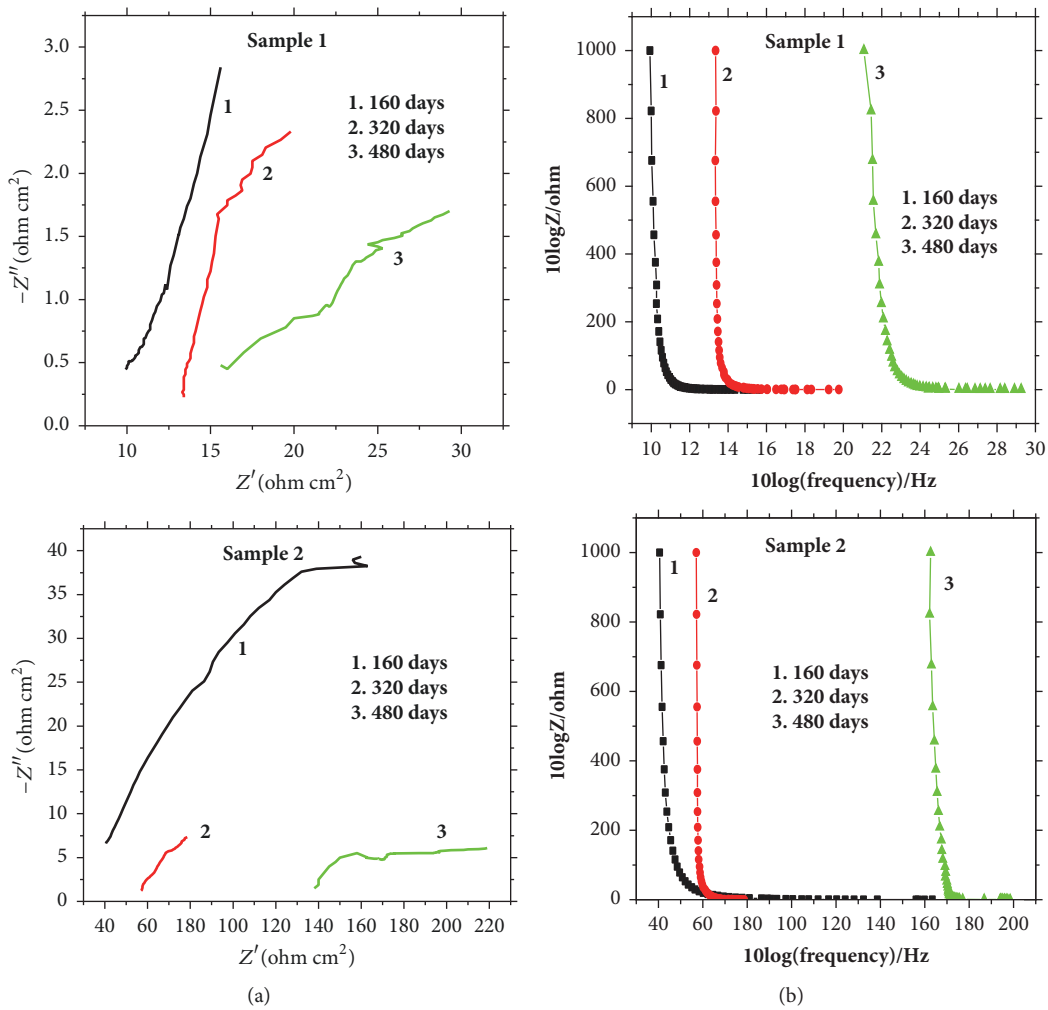


Figure 3: Nyquist plots and Bode plots of steel reinforcement in concrete (a) in the absence and (b) presence of SLS for 160, 320, and 480 days.

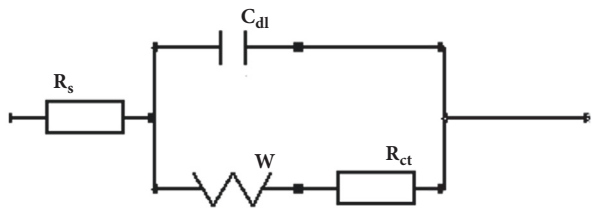


Figure 4: Equivalent circuit fitted for EIS measurements of steel reinforcement in contaminated concrete.

period of investigation. These results show that SLS is acting as a good corrosion inhibitor on steel reinforcement through the period of investigation.

*3.4. Gravimetric Analysis.* Gravimetric analysis of steel reinforcement in SAMPLE 1 and SAMPLE 2 was done for examining the percentage of weight loss and the approximate corrosion inhibition efficacy of SLS. After the period of investigation, steel specimens were taken outside from the concrete block, pickled with HCl, dried, and weighed. Steel reinforcements of SAMPLE 1 and SAMPLE 2 displayed weight losses of 24% and 3.6%, respectively. Thus the intervention of SLS on the steel rebar in concrete contaminated with NaCl was well established. Approximate value of corrosion inhibition efficiency of SLS determined by gravimetric studies was 86%.

*3.5. FT-IR Analysis.* IR spectral studies of the corroded product gave an idea about the nature of interaction of SLS on steel reinforcement. Surface deposits were removed and subjected to spectral analysis. Various compounds such as ferrous and ferric hydroxides, hydrated ferric oxide, and ferrous chloride may be deposited on the steel reinforcement. A broad signal observed at 3375 cm$^{-1}$ in the spectrum of corroded product of SAMPLE 1 was due to –OH stretching frequency of ferrous hydroxide or hydrated ferric oxide (or both) [35]. In the IR spectrum of corroded product of SAMPLE 2, it was noticed

Table 3: Half cell potential (mV) of steel reinforcement in concrete in the presence and absence of SLS for 480 days.

| **Day** | 30 | 60 | 90 | 120 | 150 | 180 | 210 | 240 | 270 | 300 | 330 | 360 | 390 | 420 | 450 | 480 |
|---|---|---|---|---|---|---|---|---|---|---|---|---|---|---|---|---|
| SAMPLE 1 | -607 | -588 | -580 | -555 | -560 | -554 | -567 | -578 | -611 | -592 | -625 | -628 | -589 | -602 | -597 | -600 |
| SAMPLE 2 | -416 | -463 | -420 | -423 | -514 | -457 | -497 | -473 | -440 | -416 | -499 | -516 | -535 | -399 | -397 | -389 |

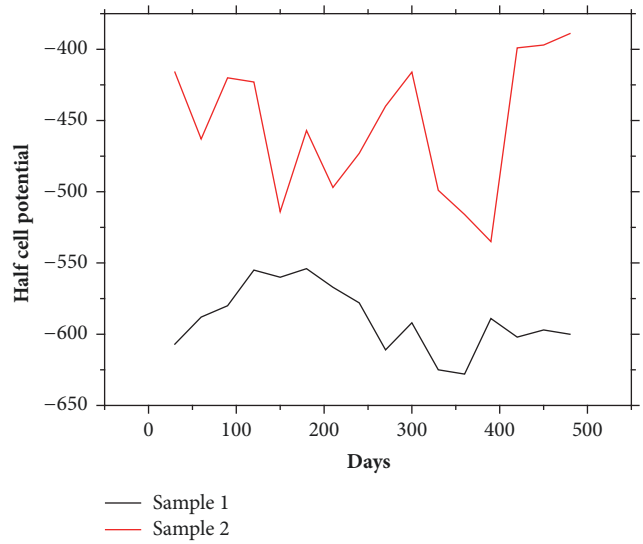


Figure 5: Variation of half cell potentials of steel reinforcement in contaminated concrete in the absence (SAMPLE 1) and presence (SAMPLE 2) of SLS during 480 days.

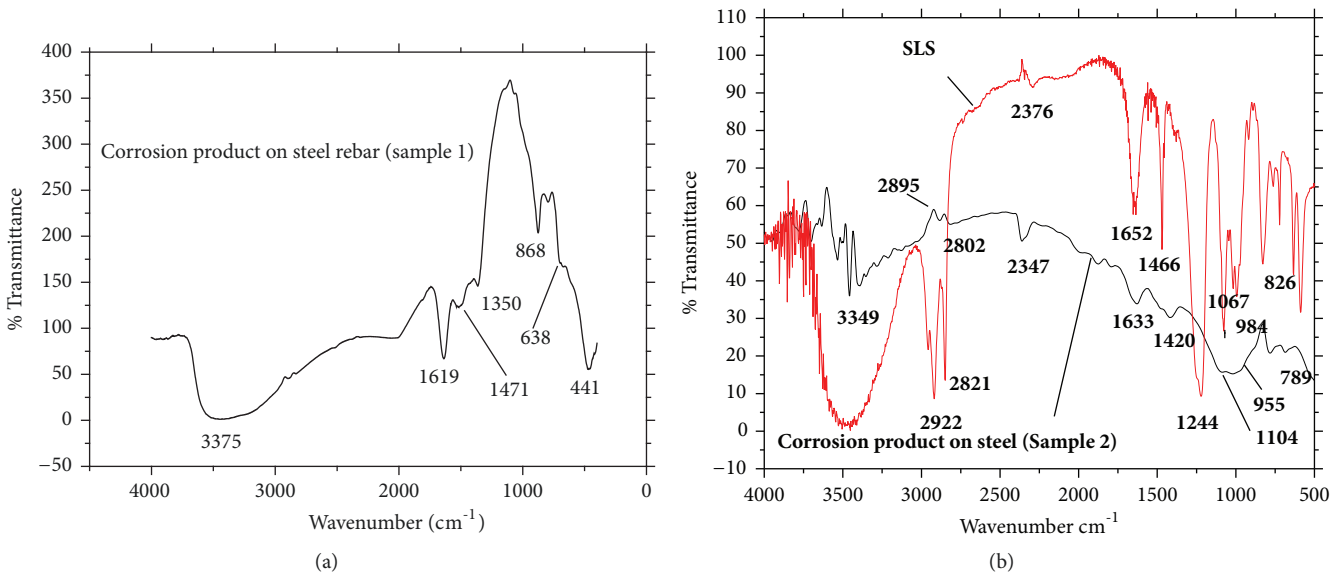


Figure 6: IR spectrum of oxide film deposited on the steel reinforcement in (a) SAMPLE 1 and (b) SAMPLE 2 and spectrum of SLS.

that the peak due to –OH frequency shifted to 3349 $cm^{-1}$. This may be due to the interaction of SLS with the ferrous or ferric hydroxide. The IR spectrum of sodium lauryl sulphate contains peaks at 2922 and 2821 $cm^{-1}$ which can assigned to the stretching frequencies of various C-H. This peak was visible at 2895 $cm^{-1}$ in the spectrum of surface product of SAMPLE 2 steel specimen. In the IR spectrum of SLS, two IR regions corresponding to symmetric and asymmetric stretching frequency of sulphate group appeared at 826-1240$cm^{-1}$ and 1240-1466$cm^{-1}$, respectively. These peaks were shifted to 789-1104$cm^{-1}$ and 1104-1420$cm^{-1}$ in the spectrum of corroded product of SAMPLE 2. This is clear indication of the interaction of SLS through the sulphate end. A weak peak corresponding to the C-C stretching frequency of carbon skeleton displayed at 964$cm^{-1}$ in the IR spectrum of SLS was shifted to 955$cm^{-1}$. Two intense peaks at 2821$cm^{-1}$ and 2922$cm^{-1}$ corresponding to symmetric and asymmetric stretching frequencies of $CH_2$ groups of SLS also shifted to 2802$cm^{-1}$ and 2895$cm^{-1}$ in the FT-IR spectrum of surface deposits of steel in SAMLE 2. Figure 6 represents the spectrum of SLS and the IR spectrum of oxide film deposited on the steel reinforcement in SAMPLE 1and SAMPLE 2.

*3.6. Microscopic Surface Analysis.* Micrographs of bare steel rebar and steel reinforcements of SAMPLE 1 and SAMPLE 2 after the investigation period are given in Figure 7. Surface of steel rebar in SAMPLE 1 contained large amount of hydrated ferric oxide. It is evident that enhanced corrosion of the


Figure 7: Optical micrographs of steel reinforcements: (a) bare, (b) in SAMPLE 1, and (c) in SAMPLE 2.

steel rebar occurred due to the continuous contact of the contaminated concrete pore solution. It was noticed that the surface of steel reinforcement in SAMPLE 2 contains little or no oxide. Thus the ability of SLS to prevent the steel reinforcement corrosion in contaminated concrete was once again proven by this analysis.

*3.7. Mechanism of Inhibition.* Sodium lauryl sulphate is a surfactant molecule and can perform well on the steel surface to decrease the rate of anodic and cathodic processes of corrosion [36, 37]. It can be assumed that SLS molecules present in concrete pore solution slowly migrate towards the steel surface and make coordinate bonds with the ferrous ions on the surface through the polar end. Since SLS has a long hydrophobic chain pointing away from the steel surface, it can repel water molecules and chloride ions diffusing towards the surface. This process is really beneficial to control the electrochemical process of corrosion. In other words, SLS efficiently resists the conversion of ferrous ions into hydrated ferric oxide (rust). The overall mechanism of the inhibition and the structure of SLS are represented in Figure 8.

## 4. Conclusion

Investigations revealed that sodium lauryl sulphate has been a potent corrosion inhibitor for the steel reinforcement in contaminated concrete for a long time. Electrochemical studies proved that the corrosion inhibition efficacy of SLS did not alter appreciably. SLS generally affect the cathodic and anodic process of corrosion. According to gravimetric studies, SLS displayed 86% of corrosion inhibition efficiency on steel reinforcement in contaminated concrete. These results are in good agreement with the electrochemical investigation results. FT-IR and microscopic surface analysis proved the interaction of SLS on steel reinforcement.

## Data Availability

No data were used to support this study.

## Conflicts of Interest

The authors declare that they have no conflicts of interest.

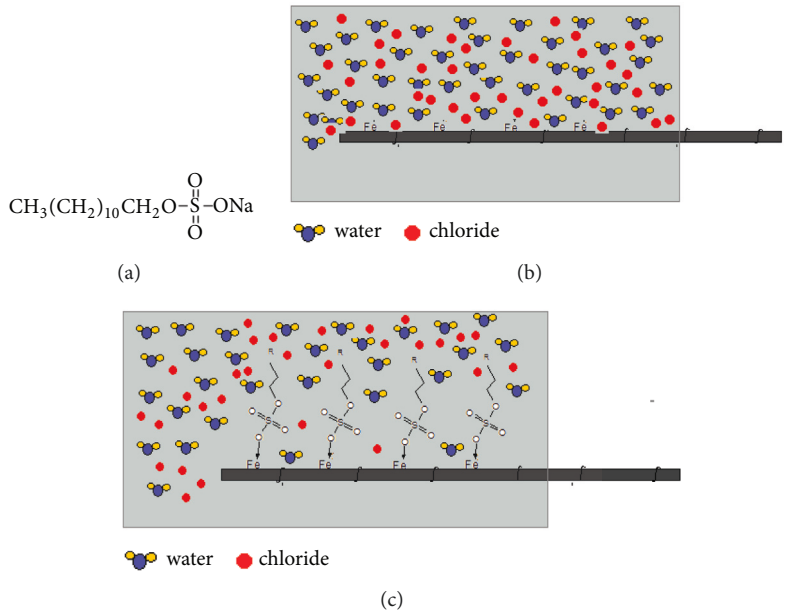


Figure 8: (a) Structure of sodium lauryl sulphate; (b) SAMPLE 1: water molecules and chloride ions are attached on steel surface; (c) SAMPLE 2: coordinated SLS prevent the migration of water molecules and chloride ions towards steel surface.

## References


[1] W. Li, C. Xu, S. Ho, B. Wang, and G. Song, "Monitoring Concrete Deterioration Due to Reinforcement Corrosion by Integrating Acoustic Emission and FBG Strain Measurements," *Sensors*, vol. 17, no. 3, p. 657, 2017.

[2] S. Ahmad, "Reinforcement corrosion in concrete structures, its monitoring and service life prediction—a review," *Cement and Concrete Composites*, vol. 25, no. 4-5, pp. 459–471, 2003.

[3] P. C. Aïtcin, "The durability characteristics of high performance concrete: a review," *Cement and Concrete Composites*, vol. 25, no. 4-5, pp. 409–420, 2003.

[4] S. Altoubat, M. Maalej, and F. U. A. Shaikh, "Laboratory Simulation of Corrosion Damage in Reinforced Concrete," *International Journal of Concrete Structures and Materials*, vol. 10, no. 3, pp. 383–391, 2016.

[5] M. F. Montemor, M. P. Cunha, M. G. Ferreira, and A. M. Simões, "Corrosion behaviour of rebars in fly ash mortar exposed to carbon dioxide and chlorides," *Cement and Concrete Composites*, vol. 24, no. 1, pp. 45–53, 2002.

[6] B. Reddy, G. K. Glass, P. J. Lim, and N. R. Buenfeld, "On the corrosion risk presented by chloride bound in concrete," *Cement and Concrete Composites*, vol. 24, no. 1, pp. 1–5, 2002.

[7] S. Nesic, J. Postlethwaite, and S. Olsen, "An Electrochemical Model for Prediction of Corrosion of Mild Steel in Aqueous Carbon Dioxide Solutions," *Corrosion*, vol. 52, no. 4, pp. 280–294, 1996.

[8] G. I. Ogundele and W. E. White, "Some Observations on Corrosion of Carbon Steel in Aqueous Environments Containing Carbon Dioxide," *Corrosion*, vol. 42, no. 2, pp. 71–78, 1986.

[9] S. M. Abd El Haleem, S. Abd El Wanees, E. E. Abd El Aal, and A. Diab, "Environmental factors affecting the corrosion behavior of reinforcing steel II. Role of some anions in the initiation and inhibition of pitting corrosion of steel in Ca(OH)2 solutions," *Corrosion Science*, vol. 52, no. 2, pp. 292–302, 2010.

[10] S. M. Abd El Haleem, S. Abd El Wanees, E. E. Abd El Aal, and A. Diab, "Environmental factors affecting the corrosion behavior of reinforcing steel. IV. Variation in the pitting corrosion current in relation to the concentration of the aggressive and the inhibitive anions," *Corrosion Science*, vol. 52, no. 5, pp. 1675–1683, 2010.

[11] M. S. Darmawan, "Pitting corrosion model for reinforced concrete structures in a chloride environment," *Magazine of Concrete Research*, vol. 62, no. 2, pp. 91–101, 2010.

[12] M. S. Anwar, B. Fadillah, A. Nikitasari, S. Oediyani, and E. Mabruri, "Study of Pitting Resistance of Rebar Steels in Jakarta Coastal Using Simulated Concrete Pore Solution," *Procedia Engineering*, vol. 171, pp. 517–525, 2017.

[13] J. G. Cabrera, "Deterioration of concrete due to reinforcement steel corrosion," *Cement and Concrete Composites*, vol. 18, no. 1, pp. 47–59, 1996.

[14] X. G. Feng, G. H. Dong, and J. Y. Fan, "Effectiveness of an inorganic corrosion inhibitor in pore solution containing sodium chloride," *Applied Mechanics and Materials*, vol. 556-562, pp. 158–161, 2014.

[15] A. U. Malik, I. Andijani, F. Al-Moaili, and G. Ozair, "Studies on the performance of migratory corrosion inhibitors in protection of rebar concrete in Gulf seawater environment," *Cement and Concrete Composites*, vol. 26, no. 3, pp. 235–242, 2004.

[16] A. M. Vaysburd and P. H. Emmons, "Corrosion inhibitors and other protective systems in concrete repair: concepts or misconcepts," *Cement and Concrete Composites*, vol. 26, no. 3, pp. 255–263, 2004.

[17] H. Oranowska and Z. Szklarska-Smialowska, "An electrochemical and ellipsometric investigation of surface films grown on iron in saturated calcium hydroxide solutions with or without chloride ions," *Corrosion Science*, vol. 21, no. 11, pp. 735–747, 1981.

[18] C. Cao, "On electrochemical techniques for interface inhibitor research," *Corrosion Science*, vol. 38, no. 12, pp. 2073–2082, 1996.

[19] S. Qian and D. Cusson, "Electrochemical evaluation of the performance of corrosion-inhibiting systems in concrete bridges," *Cement and Concrete Composites*, vol. 26, no. 3, pp. 217–233, 2004.

[20] U. Angst, B. Elsener, C. K. Larsen, and Ø. Vennesland, "Critical chloride content in reinforced concrete—a review," *Cement and Concrete Research*, vol. 39, no. 12, pp. 1122–1138, 2009.

[21] S. A. Al-Saleh, "Analysis of total chloride content in concrete," *Case Studies in Construction Materials*, vol. 3, pp. 78–82, 2015.

[22] A. Welle, J. D. Liao, K. Kaiser, M. Grunze, U. Mäder, and N. Blank, "Interactions of N,N′-dimethylaminoethanol with steel surfaces in alkaline and chlorine containing solutions," *Applied Surface Science*, vol. 119, no. 3-4, pp. 185–190, 1997.

[23] A. Królikowski and J. Kuziak, "Impedance study on calcium nitrite as a penetrating corrosion inhibitor for steel in concrete," *Electrochimica Acta*, vol. 56, no. 23, pp. 7845–7853, 2011.

[24] F. Wombacher, U. Maeder, and B. Marazzani, "Aminoalcohol based mixed corrosion inhibitors," *Cement and Concrete Composites*, vol. 26, no. 3, pp. 209–216, 2004.

[25] C. K. Nmai, "Multi-functional organic corrosion inhibitor," *Cement and Concrete Composites*, vol. 26, no. 3, pp. 199–207, 2004.

[26] J. M. Gaidis, "Chemistry of corrosion inhibitors," *Cement and Concrete Composites*, vol. 26, no. 3, pp. 181–189, 2004.

[27] P. Montes, T. W. Bremner, and D. H. Lister, "Influence of calcium nitrite inhibitor and crack width on corrosion of steel in high performance concrete subjected to a simulated marine environment," *Cement and Concrete Composites*, vol. 26, no. 3, pp. 243–253, 2004.

[28] M. A. Asaad, M. Ismail, M. M. Tahir, G. F. Huseien, P. B. Raja, and Y. P. Asmara, "Enhanced corrosion resistance of reinforced concrete: Role of emerging eco-friendly Elaeis guineensis/silver nanoparticles inhibitor," *Construction and Building Materials*, vol. 188, pp. 555–568, 2018.

[29] M. G. L. Annaamalai, G. Maheswaran, N. Ramesh, C. Kamal, G. Venkatesh, and P. Vennila, "Investigation of Corrosion Inhibition of Welan Gum and Neem Gum on Reinforcing Steel Embedded in Concrete," *International Journal of Electrochemical Science*, vol. 13, pp. 9981–9998, 2018.

[30] A. Kumar, "Corrosion Inhibition of Mild Steel in Hydrochloric Acid by Sodium Lauryl Sulfate (SLS)," *E-Journal of Chemistry*, vol. 5, Article ID 574343, 6 pages, 2008.

[31] M. L. Cedeño, L. E. Vera, and T. Y. Pineda, "A study of corrosion inhibition of steel AISI-SAE 1020 in CO 2 -brine using surfactant Tween 80," *Journal of Physics: Conference Series*, vol. 786, Article ID 12038, 2017.

[32] H. J. Flitt and D. P. Schweinsberg, "Evaluation of corrosion rate from polarisation curves not exhibiting a Tafel region," *Corrosion Science*, vol. 47, no. 12, pp. 3034–3052, 2005.

[33] J. Chen and X. Zhang, "AC impedance spectroscopy analysis of the corrosion behavior of reinforced concrete in chloride solution," *International Journal of Electrochemical Science*, vol. 12, no. 6, pp. 5036–5043, 2017.

[34] D. V. Ribeiro, C. A. C. Souza, and J. C. C. Abrantes, "Use of Electrochemical Impedance Spectroscopy (EIS) to monitoring the corrosion of reinforced concrete," *Revista IBRACON de Estruturas e Materiais*, vol. 8, no. 4, pp. 529–546, 2015.

[35] K. V. S. Ramana, S. Kaliappan, N. Ramanathan, and V. Kavitha, "Characterization of rust phases formed on low carbon steel exposed to natural marine environment of Chennai harbour - South India," *Materials and Corrosion*, vol. 58, no. 11, pp. 873–880, 2007.

[36] T. Zhao and G. Mu, "The adsorption and corrosion inhibition of anion surfactants on aluminium surface in hydrochloric acid," *Corrosion Science*, vol. 41, no. 10, pp. 1937–1944, 1999.

[37] Y. Zhu, M. L. Free, R. Woollam, and W. Durnie, "A review of surfactants as corrosion inhibitors and associated modeling," *Progress in Materials Science*, vol. 90, pp. 159–223, 2017.